OUKA
The University of Osaka
Institutional Knowledge Archive

| | |
|---|---|
| Title | Improvement in the toughness and compatibility of poly(lactic acid)/starch acetoacetate through reactive melt-kneading with amine-modified silicone |
| Author(s) | Shibasaki, Kazuki; Hsu, Yu I.; Uyama, Hiroshi |
| Citation | Polymer Journal. 2024, p. 1622 |
| Version Type | VoR |
| URL | https://hdl.handle.net/11094/100123 |
| rights | This article is licensed under a Creative Commons Attribution 4.0 International License. |
| Note | |

*The University of Osaka Institutional Knowledge Archive : OUKA*

https://ir.library.osaka-u.ac.jp/

The University of Osaka

Polymer Journal
https://doi.org/10.1038/s41428-024-00971-0

ORIGINAL ARTICLE

# Improvement in the toughness and compatibility of poly(lactic acid)/starch acetoacetate through reactive melt-kneading with amine-modified silicone

Kazuki Shibasaki[1] · Yu-I Hsu[1] · Hiroshi Uyama[1]

Received: 12 July 2024 / Revised: 23 August 2024 / Accepted: 31 August 2024
© The Author(s) 2024. This article is published with open access

## Abstract

Nonbiodegradable plastic pollution has taken centerstage because of its negative impacts on ecosystems, and poly(lactic acid) (PLA)/starch blends, which are biodegradable plastics, have attracted increased attention as sustainable materials. However, the poor compatibility between hydrophobic PLA and hydrophilic starch causes their composites to become brittle. In this study, to improve the compatibility between PLA and starch, the hydroxyl groups of starch were modified with acetoacetate, and amine-modified silicone was used as the compatibilizer. The acetoacetyl group readily reacts with primary amines under mild conditions to form enamines and is expected to react rapidly during the melt-kneading process. The amino groups also react with the decomposed PLA end groups via condensation. Therefore, amine-modified silicone is considered a suitable compatibilizer for PLA and starch acetoacetate (SAA). PLA/SAA/amine-modified silicone blends were prepared via melt-kneading. The toughness of PLA/SAA was improved by approximately 15 times when 3 wt% amine-modified silicone was added. Furthermore, in the SEM observation of the tensile fracture surface, it was found that the dispersibility of SAA in PLA was improved such that SAA and PLA were indistinguishable. This approach can contribute to the widespread use of biodegradable plastics in packaging materials and single-use plastics.

## Introduction

Petroleum-derived plastics such as polyolefins can harm ecosystems because they do not degrade easily in the natural environment. Plastic waste in the ocean increased dramatically in the 1950s with the widespread use of plastics [1, 2]. Furthermore, plastic emissions are expected to continue to increase, with annual emissions reaching 53 million tons by 2030 [3]. Biodegradable plastics are considered to have a lower environmental impact than existing petroleum-based plastics do and are therefore attracting attention as a solution to waste management and marine pollution. Biodegradable plastics undergo microbial degradation under certain environmental conditions and are converted into water, carbon dioxide, and organic matter [4]. Hence, the use of biodegradable plastics can potentially reduce the impact of plastic waste on the environment. Biodegradable plastics are particularly promising alternatives to single-use plastics such as plastic bags. Hence, the demand for the development and use of sustainable plastic materials is increasing, resulting in rapid growth in research on biodegradable plastics [5].

Typical examples of biodegradable plastics include polybutylene adipate terephthalate (PBAT) derived from petroleum, polylactic acid (PLA) derived from plants, and polyhydroxyalkanoate (PHA) derived from microorganisms. PLA is a well-known biodegradable plastic, and its main raw material is starch derived from plants such as corn and sugarcane [6, 7]. Under suitable environmental conditions (such as temperature and humidity), PLA decomposes over time and turns into water, carbon dioxide, and organic matter [8, 9]. Thus, it can help reduce plastic pollution from a waste management perspective. However, PLA has several disadvantages over traditional biodegradable plastics, such as a slow degradation rate, relatively high cost, and brittleness [10]. Furthermore, PLA does not degrade easily

**Supplementary information** The online version contains supplementary material available at https://doi.org/10.1038/s41428-024-00971-0.

✉ Yu-I Hsu
yuihsu@chem.eng.osaka-u.ac.jp

[1] Graduate School of Engineering, Osaka University, 2-1 Yamadaoka, Suita, Japan

Published online: 13 December 2024

in marine environments; therefore, there is a concern that it transforms into microplastics after it enters marine environments [11]. To resolve this issue, the marine biodegradability of PLA must be increased.

Starch is one of the most abundant natural polysaccharides synthesized in plants. In contrast to PLA, starch degrades in any environment, such as in oceans and soil. It is the main component of biopolymer structures in the polysaccharide group and is considered the second most important renewable resource after cellulose [12]. In recent years, starch-based plastic materials have attracted considerable attention owing to their sustainable nature [13–15]. Starch is composed of two components: linear amylose with α-1–4 bonds between the glucose monomers and branched amylopectin with both α-1-4 and α-1-6 bonds [16]. Starch does not exhibit thermoplasticity because of the strong intra- and intermolecular hydrogen bonds between its hydroxyl groups [17]. Therefore, starch is used as thermoplastic starch (TPS) with plasticizers in composites with other biodegradable plastics. Adding plasticizers such as glycerol or sorbitol to starch decreases the number of hydrogen bonds within the starch and increases its molecular mobility, and the starch becomes thermoplastic starch [18, 19].

Many studies have reported the use of thermoplastic starch composites with biodegradable plastics to achieve high performance and low cost. Starch is expected to improve the marine biodegradability of plastics [20]. Thus, blends of PLA and TPS have potential for a wide range of applications in agriculture, the packaging industry, and biomedical fields as biodegradable marine materials. In addition, blends of PBAT and TPS have the same benefits and significant cost reductions compared with PBAT alone [21]. However, TPS is hydrophilic and incompatible with hydrophobic PLA, which degrades the mechanical properties of PLA [22]. Therefore, acetylation and maleic acid modification are used to improve the compatibility of starch with PLA by replacing the hydroxyl groups in starch [23, 24]. However, modified starch is brittle, and blending it with PLA does not significantly improve its mechanical properties.

In this study, to improve the compatibility between PLA and starch and reduce the brittleness of their blends, acetoacetate modification was used to obtain a reactive modified starch. Acetoacetyl groups react with primary amines under mild conditions without catalysts to form enamines, which were then used to synthesize vitrimers and responsive polymers [25, 26]. Acetoacetate-modified polymers have also been found to be biocompatible and are considered nature-friendly polymers [27]. This high reactivity was effectively utilized to improve the compatibility between PLA and starch acetoacetate (SAA). Specifically, amine-modified silicone was added as a compatibilizer to the PLA/SAA blends. The PLA/SAA blends were prepared by melt-kneading, during which the amine-modified silicone reacted with SAA to form dynamic enamine covalent bonds. Amine-modified silicones also reacted with the decomposed PLA end groups during heating via condensation. Therefore, amine-modified silicone reacted with both PLA and SAA to form covalent bonds, which is expected to improve the interfacial affinity between the two materials. The addition of silicone, a flexible polymer with biocompatibility and heat resistance [28, 29], is also expected to improve the flexibility of PLA/SAA. Furthermore, silicone does not emit carbon dioxide when disposed of, so its use helps reduce its environmental impact in light of global warming issues. Hence, this blended material is promising for applications in the food packaging and biomedical fields. In this study, the mechanical properties of PLA/SAA with amine-modified silicone and the mechanical effects of the viscosity of amine-modified silicone and the position of the amine modification in silicone on PLA/SAA were evaluated. In addition, thermal and crystal structure analyses, morphological observations and biodegradability studies in the ocean atmosphere were performed to develop a deeper understanding of the mechanical properties of the material.

## Experimental section

### Materials

PLA (2003D) was supplied by NatureWorks, LLC (Minnesota, USA). The melt flow rate (MFR) was 6 g/10 min (210 °C, 2.16 kg). Native cornstarch and thermoplasticized starch (TPS) were obtained from Matsutani Chemical Industry Co., Ltd. (Hyogo, Japan) and Sankyo Chemical Industry Co., Ltd. (Osaka, Japan), respectively. Tert-butyl acetoacetate (t-BAA) was supplied by Tokyo Chemical Industry Co., Ltd. (Tokyo, Japan). The silicone samples listed in Table 1 were obtained from Shin-Etsu Chemical Co., Ltd. (Tokyo, Japan). Silicones with the end group in the modified position are bifunctional amine-modified silicones, whereas silicones with the side chain in the modified position are multifunctional amine-modified silicones. The

**Table 1** Sample information for silicone

| Sample | Amino group equivalent [g/mol] | Modification position | Viscosity @25 °C [cs] |
|---|---|---|---|
| PDMS | - | - | 50 |
| End800 | 800 | End group | 25 |
| End1500 | 1500 | End group | 55 |
| End5700 | 5700 | End group | 450 |
| Side3800 | 3800 | Side chain | 1700 |

**Table 2** Composition of PLA/SAA/silicone blend

| Sample | PLA [wt%] | TPS [wt%] | SAA [wt%] | Silicone [phr] |
|---|---|---|---|---|
| PLA/TPS | 80 | 20 | – | – |
| PLA/SAA | 80 | – | 20 | – |
| PLA/SAA/PDMS | 80 | – | 20 | 3 |
| PLA/SAA/End800 | 80 | – | 20 | 3 |
| PLA/SAA/End1500 | 80 | – | 20 | 3 |
| PLA/SAA/End5700 | 80 | – | 20 | 3 |
| PLA/SAA/Side3800 | 80 | – | 20 | 3 |

length of the silicone chain per mole of amine is also indicated by the amine group equivalent. For example, End800 is bifunctional, so it has a silicone chain length of 1600 g/mol. Polydimethylsiloxane (PDMS) was prepared for comparison with amine-modified silicone. All the reagents were used without further purification.

## Synthesis procedure of SAA

SAA (degree of substitution = 1.57) was synthesized as previously reported [30, 31]. Starch (10.0 g, anhydroglucose unit: 61.7 mmol) was added to 200 ml of dimethyl sulfoxide (DMSO) in a three-necked flask. The mixture was heated to 90 °C to completely dissolve the starch. Then, t-BAA (51.2 ml, 0.31 mol) was added dropwise under a nitrogen atmosphere, and the reaction was carried out at 120 °C for 2 hours. After the reaction, the SAA mixture was obtained by reprecipitation in ethanol. Pure SAA was obtained by washing with acetone to remove unreacted t-BAA, followed by drying under vacuum.

The structure of SAA was confirmed via proton nuclear magnetic resonance ($^1$H-NMR) (Bruker AVANCE III 600 MHz, Bruker Corporation, Massachusetts, USA) using deuterated dimethyl sulfoxide (DMSO-$_{d6}$) as the solvent.

## Preparation of PLA/SAA with amine-modified silicone blends

The compositions of the blends are listed in Table 2. Blends with more than 5 wt% PDMS or amine-modified silicone with high amine functional group equivalents exhibited phase separation and could not be formed into films. Therefore, blends with 3 wt% silicone are reported in this study. PLA/SAA with silicone blends were prepared via melt-kneading via a twin-screw internal mixer (Labo Plastmill 4C150-01; Toyo Seiki Co., Ltd., Osaka, Japan). Before blending, the PLA, TPS, and SAA samples were dried under vacuum at 80 °C for 4 h to remove water. To prepare the PLA/TPS and PLA/SAA blends, PLA was blended with TPS or SAA at 170 °C with a screw speed of 70 rpm for 10 min. To prepare the PLA/SAA and amine-modified silicone blends, PLA and SAA were blended at 170 °C with a screw speed of 70 rpm for 3 min. Silicone was then added and kneaded to the same temperature at a screw speed of 20 rpm for 7 min.

The 0.5 mm thick blend films were molded by hot-pressing at 180 °C for 5 min at 20 MPa and quenched with ice. An Izod impact sample with a thickness of 4 mm was prepared via an injection molding machine (HAAKE MiniJet Pro, Thermo Fisher Scientific Inc., Massachusetts, USA) by melting blended samples in a cylinder at 185 °C for 10 min and extruding them at 750 bars into a mold (80 × 10 × 4 mm) at 45 °C.

## Measurement

Differential scanning calorimetry (DSC) measurements (NEXTA DSC200, Hitachi High-Tech Corporation, Tokyo, Japan) were performed to evaluate the thermal properties of the blended films. The samples were measured within a temperature range of −40–180 °C up to the 2nd heating curve at a rate of 10 °C/min. Nitrogen at a flow rate of 40 mL/min was used as the atmosphere.

Wide-angle X-ray diffraction (WAXD) was performed at beamline BL40B2 in the SPring-8 Synchrotron Radiation Facility (Sayo, Japan). Before the measurements, the blended samples were annealed at 110 °C for 2 h to evaluate the crystal structure. The blend films were irradiated for 3 s at a wavelength of 0.1 nm, and 2D images were recorded via the detectors. A flat panel (C9728DK-10; Hamamatsu Photonics KK, Shizuoka, Japan) was used as the WAXD detector. The sample-to-detector length of the WAXD profiles was 58.3 mm.

The sample mechanical properties were evaluated via tensile and Izod impact tests. Tensile tests were performed via an AutoGraph AGS-X (Shimazu Corporation, Kyoto, Japan) at a constant deformation rate of 10 mm/min. The samples were cut into dumbbell-shaped sheets (W 4 mm × D 20 mm) of approximately 0.5 mm. Ichod impact tests were performed via an Izod impact tester (IM-1110; UESHIMA SEISAKUSHO Co., Ltd., Tokyo, Japan). The samples were notched to a depth of 2 mm via a notching machine (C-6898-000; Instron Co., Ltd., Massachusetts, USA).

The morphologies of the fracture surfaces of the blended samples were observed by scanning electron microscopy (SEM) (SU3500, Hitachi High-Tech Corporation, Tokyo, Japan) at an acceleration voltage of 10.0 kV. The samples were coated with a platinum sputter (MSP-1S, VACUUM DEVICE Co., Ltd., Ibaraki, Japan) before being loaded into the SEM device.

The biodegradability of the PLA/SAA/silicone blends in marine environments was assessed via biochemical oxygen demand (BOD) testing in accordance with OECD 306. Seawater was collected from the sea in Hyogo Prefecture (34°71'N, 135°35'E). Seawater was collected on October 1, 2023, with a water temperature of 22.2 °C. The tests were conducted in a pressure sensor-type BOD reactor (6D, TAITEC Co., Ltd., Saitama, Japan) in the dark at 20 °C for 28 days. Aniline was used as a reference. The samples evaluated were PLA, PLA/TPS, PLA/SAA and PLA/SAA/End800 as representative samples containing silicone. Each BOD reactor contained 10 mg of aniline and a 10x10x0.5 mm thick sample film, along with 100 ml of seawater and nutrients (25 mg of $NH_4Cl$, 5 mg of $NaHPO_4$, 0.5 mg of N-allylthiourea, and 0.1 mL of a buffer solution) to ensure unrestricted conditions for microbial activity and growth. Equation (1) was used to calculate the BOD biodegradability. $BOD_s$ represent the BOD of the sample, whereas $BOD_{blank}$ represents the BOD of a reactor that contained nothing. ThOD refers to the theoretical oxygen demand.

$$\mathrm{BOD}\,(\%) = \frac{\mathrm{BOD_s} - \mathrm{BOD_{blank}}}{\mathrm{ThOD}} \times 100 \quad (1)$$

## Results and discussion

### Characterization of SAA

The $^1$H-NMR spectra of native corn starch and SAA are shown in Fig. 1. The peaks of the protons of the anhydroglucose unit showed chemical shifts (δ) of 3.0–4.0 ppm and 5.0–5.2 ppm [32]. In contrast, the anhydroglucose unit-derived peaks were broader for SAA than for starch. Furthermore, SAA presented new peaks at δ 3.6 ppm and 2.2 ppm. The peak at δ 3.6 ppm was attributed to methylene, and the peak at 2.2 ppm was attributed to the methyl group of the acetoacetate group. These results indicated that a portion of the hydroxyl groups in the starch were modified by acetoacetyl groups [30]. The degree of substitution (DS) as calculated from $^1$H-NMR was 1.57. This was calculated via Equation (2), consistent with Weng et al. [31]. Here, the integration of the total area of anhydroglucose includes the methylene-derived integral of the acetoacetyl group. To remove the integration, the ratio of the acetoacetyl group to the methyl group (0.67) was subtracted from this integration. Seven and three are the numbers of protons on the anhydroglucose units and the numbers of methyl groups of the acetoacetyl groups, respectively.

$$\mathrm{DS} = \frac{(\text{Integration of peak a}) \times 7}{(\text{Integration of total area of anhydroglucose units} - 0.67) \times 3} \quad (2)$$

The thermal properties of the samples were confirmed via DSC. The 2nd heating curves for native corn starch and SAA are shown in Fig. 2. Native corn starch did not have a glass transition temperature (Tg), whereas SAA had a Tg at

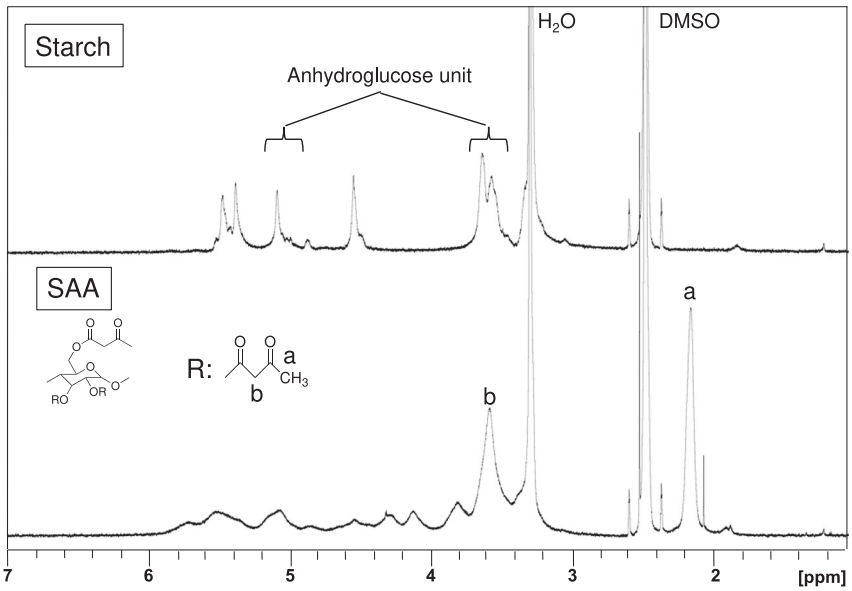


**Fig. 1** $^1$H-NMR spectra of native corn starch and SAA in DMSO-$_{d6}$

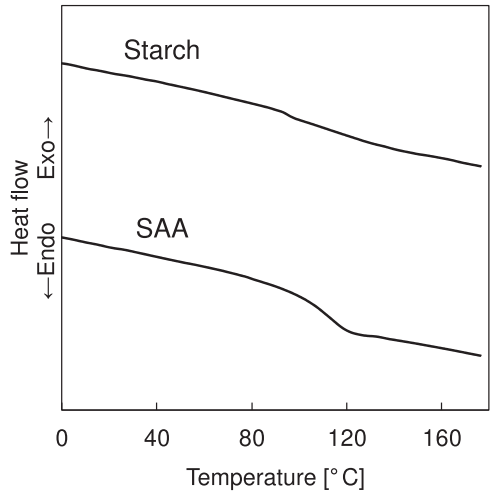


**Fig. 2** DSC 2nd heating curves of native starch and SAA

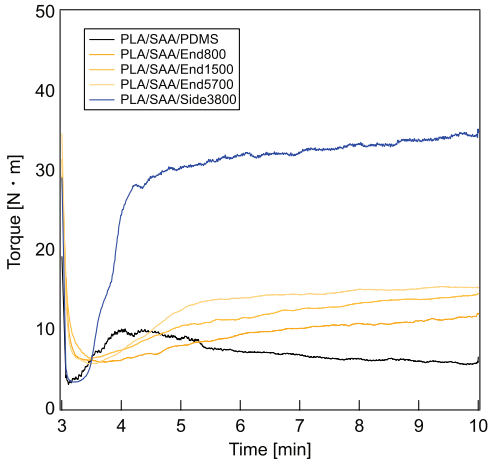


**Fig. 3** Change in torque with time after the addition of amine-modified silicone

113 °C, indicating that it has thermoplasticity above 113 °C. Native cornstarch has intra- and intermolecular hydrogen bonds and does not exhibit thermoplasticity [17, 33]. Therefore, plasticizers, such as water or glycerol, have been added to improve the thermoplasticity of starch. Furthermore, the DSC curve of the SAA did not show a crystallization temperature (Tc) or melting point (Tm), indicating that SAA is an amorphous thermoplastic polymer. This thermoplasticity is due to acetoacetate groups that are modified by the transesterification of hydroxy groups in starch, which reduces the number of hydroxyl groups in starch, providing steric hindrance and thus relaxing hydrogen bonds. As this behavior has also been reported for other modified starches, the degree of relaxation of intramolecular hydrogen bonds, that is, the degree of substitution, is considered to depend on the glass transition temperature [30].

## Behavior of PLA/SAA/amine-modified silicone during melt-kneading

PLA/SAA/amine-modified silicone blends were prepared by melt-kneading at 170 °C for 10 min. During the preparation of the blend sample, the torque value of the screw rotation changed during melt-kneading after amine-modified silicone was added to the PLA/SAA blend (Fig. 3). For PLA/SAA/PDMS, the torque increased after the addition of PDMS and then decreased slowly. The initial increase in torque is attributed to the homogeneous mixing of PLA and PDMS. The gradual decrease in torque is assumed to be due to the thermal decomposition of PLA [34]. In contrast, the torque increased slowly in the sample with amine-modified silicone after the amine-modified silicone was homogeneously dispersed in the PLA matrix. SAA forms dynamic covalent bonds with amine-modified silicone (Fig. 4a). This reaction was supported by FTIR measurements of SAA and amine-modified silicone in the component system (Fig. 1S). On the other hand, the compatibility of PLA with SAA and amine-modified silicone was likely enhanced by polar interactions due to the acetoacetyl groups derived from SAA and the enamine structure and by the condensation reaction between the PLA termini that were thermally decomposed during kneading and the amine-modified silicone (Fig. 4b). The amine-modified silicone acted as a crosslinker, and an SAA/amine-modified silicone crosslinked structure was considered to have formed within the PLA matrix. The formation of crosslinked structures and the recombination of thermally decomposed PLA were attributed to an increase in melt viscosity [35]. The initial torque increase (3–5 min) was considered to depend on the viscosity of the amine-modified silicone. PLA/SAA/Side3800 had a higher torque when the amine-modified silicone was homogeneously dispersed within the PLA because of the extremely high viscosity of the amine-modified silicone compared with that of the other samples. Except for Side3800, PLA/SAA/End800 had the greatest change (0.58 N・m/min) in torque with time for mixing times of 8–10 min, whereas PLA/SAA/End5700 had the lowest change (0.22 N・m/min). This finding indicates that the more amino groups there are, the more densely cross-linked the structure.

## Thermal properties and crystal structure of the blended samples

DSC measurements were performed to evaluate the effects of adding amine-modified silicone to PLA/SAA on the Tg, Tc, Tm and crystallinity ($\chi$) of PLA (Fig. 5). The measurement results of the 2nd heating, transition temperature, and crystallinity are summarized in Table 3. The crystallinity was calculated via Eq. (3) to include cold

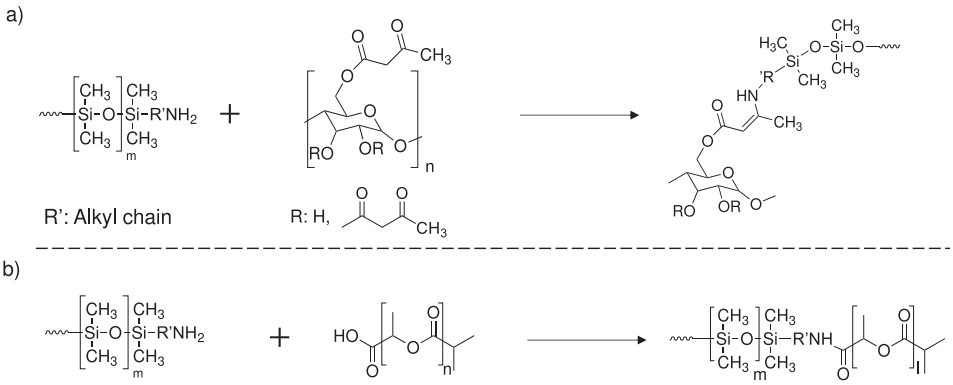


**Fig. 4** Schematic illustration of the proposed reaction between (**a**) SAA and amine-modified silicone and (**b**) PLA and amine-modified silicone

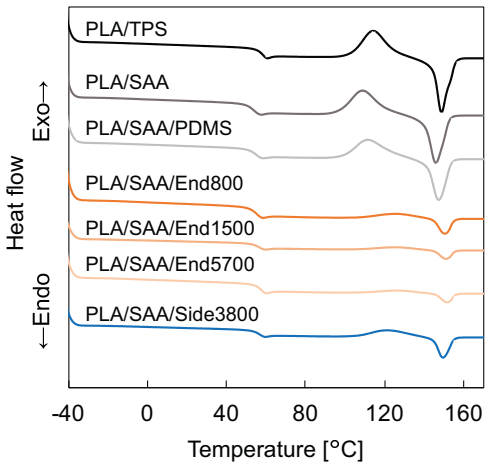


**Fig. 5** DSC 2nd heating curves of the PLA/SAA/silicone blends

crystallization, where ΔH is the melting enthalpy of the blend sample and where $\Delta H_m^0$ is the equilibrium melting enthalpy of PLA, 93.1 J/g [36].

$$\chi = \frac{\Delta H_m}{\Delta H_m^0} \times 100 \tag{3}$$

The crystallinity of the PLA/TPS and PLA/SAA blends was found to be greater than that of PLA, which likely occurred because the starch component acted as a crystal-nucleating agent for PLA [37, 38]. PLA/TPS showed slightly higher crystallinity than did PLA/SAA, which was due to the presence of the plasticizer glycerol in TPS. Crystallinity was considered to have been increased by the increased molecular mobility of PLA in the crystallization temperature region with the introduction of the plasticizer [39]. The addition of PDMS to PLA/SAA did not change the crystallinity of PLA. It was assumed that there was no interaction or reaction between PLA/SAA and PDMS because both PLA and SAA are polar polymers, whereas PDMS is a nonpolar polymer. Furthermore, because PDMS is not reactive, no factors interact with PLA/SAA. In

**Table 3** Transition temperatures and crystallinities of the PLA/SAA/silicone blends

| Sample | Tg [°C] | Tc [°C] | Tm [°C] | Crystallinity [%] |
|---|---|---|---|---|
| PLA/TPS | 57.1 | 114.2 | 148.9 | 30.0 |
| PLA/SAA | 52.7 | 108.7 | 146.1 | 26.6 |
| PLA/SAA/PDMS | 54.2 | 111.4 | 147.5 | 25.1 |
| PLA/SAA/End800 | 54.0 | 125.9 | 150.6 | 6.6 |
| PLA/SAA/End1500 | 55.6 | 125.2 | 151.0 | 6.5 |
| PLA/SAA/End5700 | 56.3 | 126.9 | 151.5 | 4.6 |
| PLA/SAA/Side3800 | 55.5 | 121.0 | 149.7 | 14.0 |

contrast, the addition of amine-modified silicone to PLA/SAA significantly reduced the crystallinity of PLA. Furthermore, in comparison with PLA/SAA, the samples with amine-modified silicone increased the crystallization temperature by approximately 10 °C. This was attributed to the formation of a cross-linked structure within the PLA matrix via the reaction between the amine-modified silicone, SAA, and PLA, which prevented the crystallization of PLA. The formation of cross-linked structures restricts the molecular mobility of PLA and inhibits its crystallization. This is supported by the increase in the crystallization temperature [40]. The correlation between the position of the modified amine in silicone and the crystallinity of PLA showed that end group modification of silicone inhibited PLA crystallization more strongly than side chain modification did, regardless of the amino group equivalent or the viscosity of silicone. It has been suggested that end group modification is more efficient for forming crosslinked structures than side chain modification in terms of conformation. For example, in side chain modification, the mobility of the remaining polymer chain is largely limited when a new bond is formed in the middle of a molecule chain. This results in less freedom in the polymer chain than does end group modification. As a result, the side chain amine-modified silicones reacted more frequently with acetoacetyl groups on the surface of the same SAA granules, and fewer molecular

chains were considered to connect SAA granules to SAA granules.

WAXD measurements were performed on PLA blended with SAA and silicone to evaluate the effect of the formation of cross-linked structures on the crystal structure of PLA. The WAXD profiles are shown in Fig. 6. PLA is now known to crystallize in three different crystal formations: α-type, β-type, and γ-type [41]. Among the three crystal forms, the α form is the crystal structure most commonly observed in crystals melt-crystallized at a Tc above 110 °C. Neat PLA showed amorphous, wide, hollow and α-crystal-derived peaks at $q = 11.5\ \mathrm{nm}^{-1}$ and $13.2\ \mathrm{nm}^{-1}$. These peaks are characterized as (110)/(200) and (203) α-crystals, respectively [42]. In the PLA/TPS and PLA/SAA blends, the crystal-derived peaks were more obvious than those in PLA. In addition, small peaks such as (203), (004)/(103), and (211), which are also derived from the α-crystal of PLA, were newly observed [43, 44]. This likely occurred because the starch component acted as a crystal-nucleating agent for PLA. This result was consistent with the crystallinity calculated via DSC. Furthermore, no peak shift of the α-crystal was observed, suggesting that TPS and SAA are not included in the crystal structure of PLA. Additionally, no shift in the α-crystal-derived peaks was observed with the addition of PDMS or End800. Therefore, silicone was considered to have been excluded from the lamellar crystals during PLA crystallization.

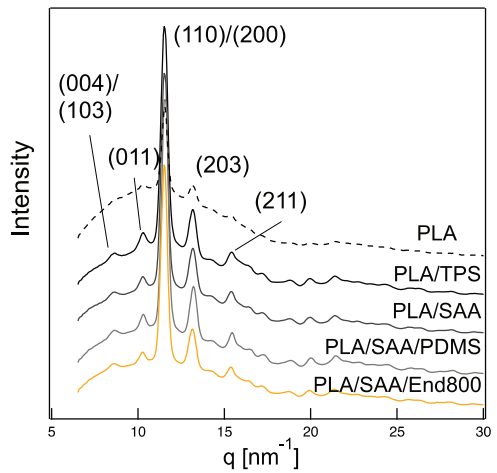


**Fig. 6** WAXD profiles of the PLA, PLA/TPS and PLA/SAA/silicone blends

## Mechanical properties of PLA/SAA/amine-modified silicone

The tensile properties and impact strengths of the samples are summarized in Table 4, where toughness is the integral of the stress–strain curve. PLA/TPS and PLA/SAA exhibited low breaking strains, which were attributed to the low compatibility of PLA, TPS, and SAA. After the addition of PDMS, the strain at break of PLA/SAA improved slightly and exhibited plastic deformation. Silicone, which has high molecular mobility at room temperature, was considered to disperse stress when tensile stress was applied. However, the addition of a small amount (3 phr) of amine-modified silicone to PLA/SAA significantly improved its mechanical properties, especially the strain at break. The PLA/SAA/End800 blend exhibited the highest toughness, which was 15 times greater than that of PLA/SAA. In addition, the Young's modulus decreased with the addition of amine-modified silicone. This suggested that the effects of SAA and TPS as fillers decreased and that they were compatible with PLA. Furthermore, amine-modified silicone effectively improved mechanical properties and had greater toughness than did PLA/SAA/PDMS. Amine-modified silicone was considered to act as a compatibilizer for PLA and SAA, and the reactions between amine-modified silicone, PLA, and SAA were also expected to form a cross-linked structure in PLA with SAA as the cross-linking points. This hypothesis is supported by the increase in the impact strength of PLA/SAA with the addition of amine-modified silicone. Compared with PLA/SAA, PLA/SAA/PDMS had slightly greater impact strength. It was assumed that the silicone with high molecular mobility dispersed in PLA/SAA dissipated energy. Compared with that of PDMS, the impact strength of PLA/SAA with amine-modified silicone was improved. The highest impact strength was observed for PLA/SAA/End800, which had the highest amine group content, and as the amine group content

**Table 4** Results of tensile tests and Izod impact tests of PLA/SAA/silicone

| Sample | Young's modulus [MPa] | Maximum stress [MPa] | Strain at break [%] | Toughness [MPa/m$^2$] | Impact strength [MPa] |
|---|---|---|---|---|---|
| PLA/TPS | 2573.9 ± 46.7 | 50.3 ± 0.7 | 2.4 ± 0.1 | 92.3 ± 12.2 | 2.84 ± 0.31 |
| PLA/SAA | 2350.4 ± 26.8 | 45.9 ± 2.1 | 2.5 ± 0.1 | 63.6 ± 9.0 | 3.62 ± 0.10 |
| PLA/SAA/PDMS | 2323.9 ± 140.3 | 34.7 ± 1.7 | 9.3 ± 2.6 | 277.2 ± 36.4 | 4.16 ± 0.04 |
| PLA/SAA/End800 | 1914.7 ± 69.2 | 27.1 ± 1.9 | 46.5 ± 8.0 | 1003.9 ± 171.2 | 6.14 ± 0.48 |
| PLA/SAA/End1500 | 2282.7 ± 30.5 | 32.8 ± 2.4 | 35.1 ± 6.2 | 917.7 ± 243.5 | 5.68 ± 0.08 |
| PLA/SAA/End5700 | 1926.4 ± 95.5 | 35.1 ± 2.8 | 7.4 ± 0.9 | 182.5 ± 4.1 | 5.17 ± 0.19 |
| PLA/SAA/Side3800 | 2162.7 ± 327.0 | 33.5 ± 2.6 | 4.2 ± 0.6 | 109.2 ± 7.2 | 5.29 ± 0.79 |

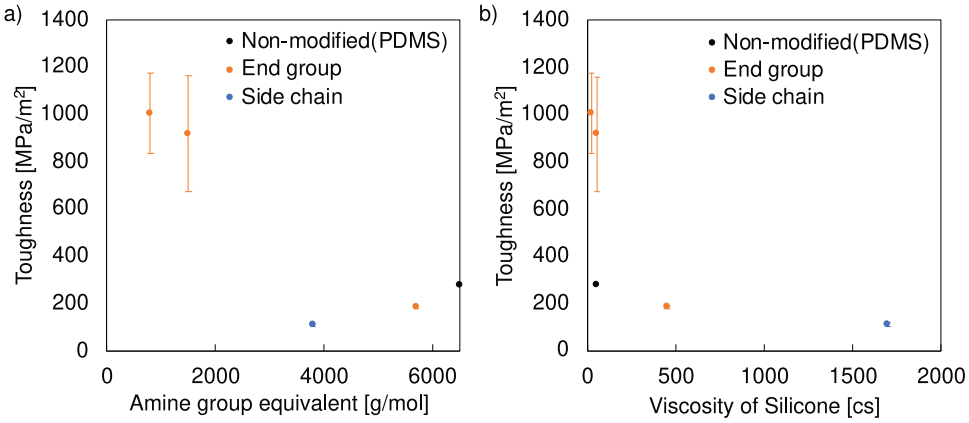


**Fig. 7** Toughness dependence of the (**a**) amine group equivalent and (**b**) viscosity of silicone

decreased, the impact strength decreased to the same level as that of PLA/SAA/PDMS. These results show that the number of amine groups in the blend has a significant effect on impact strength, which indicates the rate of formation of cross-linked structures.

Figure 7 shows the relationships among amine-modified silicone with different amine group equivalents, viscosities, and toughness values of the blend. In terms of the relationship between the amine equivalent and toughness (Fig. 7a), the toughness of the blends with end group amine-modified silicone decreased with increasing amine group equivalents. This behavior was also the same for the strain at break and impact strength of the blends, as shown in Table 4. Considering that the same weight of amine-modified silicone was added, the increase in the number of amine group equivalents resulted in a relative reduction in the number of amine groups and a decrease in the number of reaction points with SAA and PLA. A strong correlation was found between the number of amine group equivalents and the number of amino groups in blends that reacted with SAA. When the amine content was low, for example, 5000 g/mol amine equivalent, SAA was not effective as a compatibilizer and resulted in lower toughness than did the addition of PDMS. PLA/SAA/Side3800 exhibited lower toughness than did PLA/SAA/End5700, despite having a lower amine group equivalent. This suggested that side chain amine-modified silicones react more frequently with the same SAA granules and are less likely to form cross-linked structures than are the end group amine-modified silicones. This result is consistent with the crystallinity results. On the other hand, as indicated by the relationship between the viscosity of the amine-modified silicone and toughness (Fig. 7b), the toughness of the blends strongly depended on viscosity, and the toughness of the blends decreased exponentially with increasing viscosity of the amine-modified silicone, regardless of the position of the amine modification. Thus, toughness was found to be more strongly correlated with the viscosity of silicone than with the amine group equivalent or the modification position. This behavior may be related to the dispersibility of the amine-modified silicone during melt-kneading. The high viscosity of the amine-modified silicone is expected to cause phase separation within the PLA and prevent its reaction with the SAA. As a result, the toughness of PLA/SAA/End5700 and PLA/SAA/Side3800 was lower than that of the other samples.

## Morphology of the PLA/SAA/amine-modified silicone

The results of the SEM observations of the fracture section surface following the tensile test are shown in Fig. 8. Granules of TPS or SAA and the interface between PLA and TPS or SAA were observed in PLA/TPS and PLA/SAA. The fractures indicated the poor compatibility of PLA with TPS and SAA, which resulted in brittleness. Large SAA granules were observed in the PLA/SAA/PDMS samples. This morphology was attributed to the low dispersibility of SAA caused by the low melt viscosity of PLA with the addition of PDMS.

However, in PLA/SAA/End800, where the toughness was the highest, the dispersion of SAA greatly improved, and the interface between SAA and PLA became obscure. It was found that amine-modified silicone acted as a compatibilizer between PLA and SAA. This relaxed the fracture caused by stress concentration at the interface between the PLA and SAA and improved the mechanical properties of the blend. Compared with PLA/SAA/End800, PLA/SAA/End1500 and PLA/SAA/End5700 presented few SAA granules, indicating that they were not sufficiently compatible because of the lack of amino groups in silicone. This morphology was supported by its mechanical properties. The dispersibility of SAA was greater with the addition of the end group amine-modified silicone than with the addition of the side chain amine-modified silicone. Furthermore, the SAA granules formed with the addition of end group amine-modified silicone were smaller than those with the addition of side chain amine-modified silicone. The end

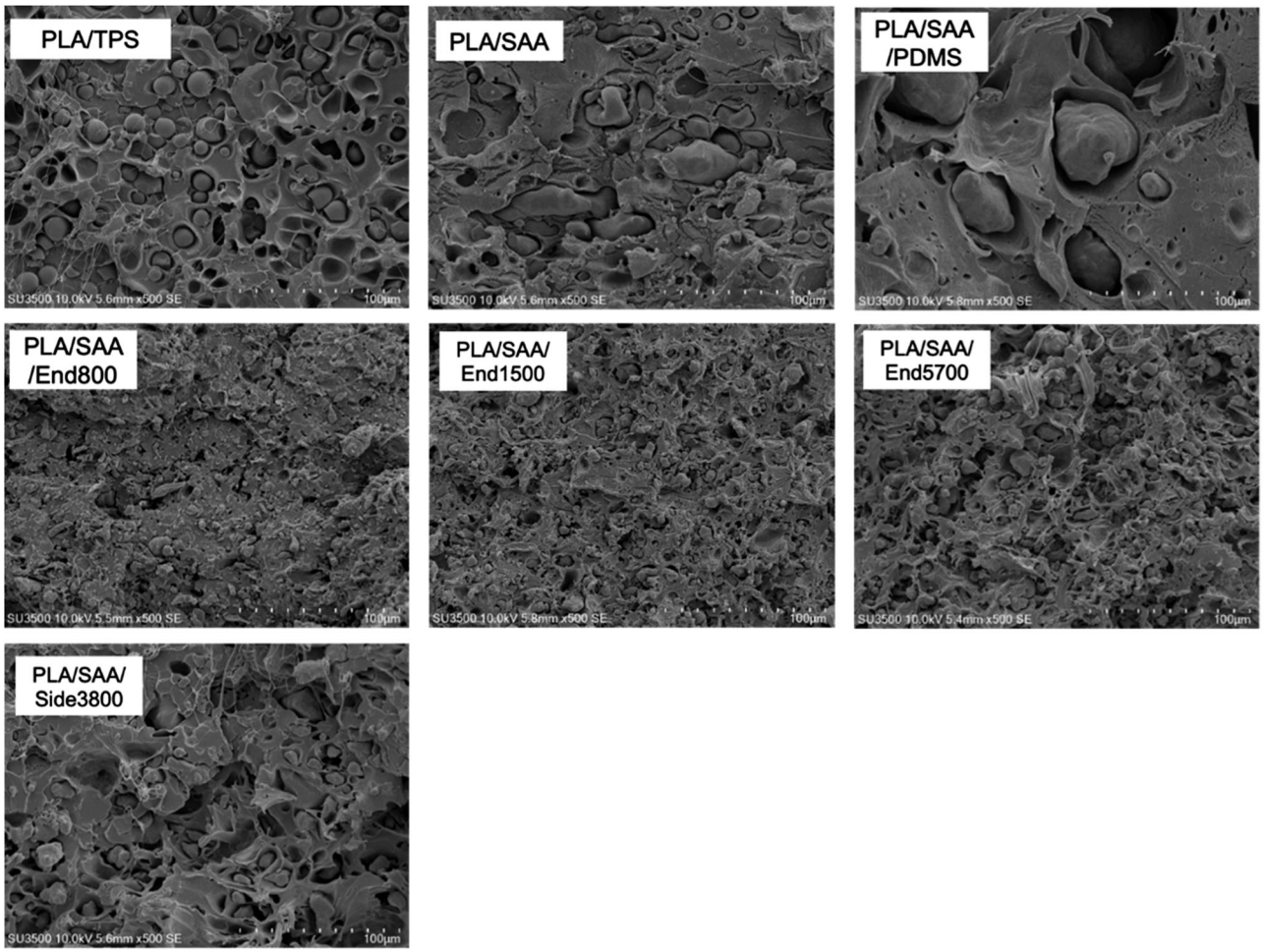


**Fig. 8** SEM images of the tensile fracture surfaces of the PLA/SAA/amine-modified silicone blends

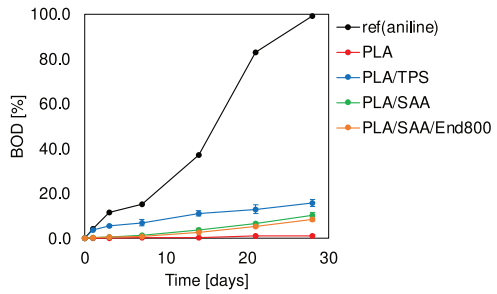


**Fig. 9** BOD test of PLA/starch and PLA/SAA/amine-modified silicone

group of the amine-modified silicone is considered to be more reactive with SAA. This result is supported by the crystallinity of PLA as calculated via DSC measurements.

## Biodegradability of PLA/SAA/silicone blends in seawater

Figure 9 shows the results of the BOD test for PLA, PLA/TPS, PLA/SAA and PLA/SAA/End800. The BOD of aniline reached 99.0% after 28 days, indicating the activity of the microorganisms during this period. The BOD values after 28 days were 1.3% for PLA, 15.8% for PLA/TPS, 10.2% for PLA/SAA, and 8.6% for PLA/SAA/End800. These results are consistent with those of previous studies showing that PLA is not biodegradable in either seawater or freshwater [45]. These findings suggest that marine spills of PLA alone could be a source of marine plastics. On the other hand, PLA/TPS exhibited the highest level of biodegradability. The BOD of TPS was 10.2% (starch: 7.3%, glycerol 1: 2.9%) when it was completely biodegraded. Therefore, the remaining 5.6% BOD was considered to be associated with the biodegradation of PLA. This value was greater than that of PLA, indicating that the coexistence of PLA with starch clearly promoted the marine biodegradability of PLA. Marine microorganisms readily degrade TPS, creating a microbe-rich environment for the blend film. This exposure caused PLA to biodegrade faster due to increased exposure to seawater and microorganisms. This behavior is similar to the biodegradability of PLA/TPS in

soil reported by Palai et al. [46]. PLA/SAA exhibited a slower initial biodegradation rate than did PLA/TPS. This is because the starch was modified with acetoacetyl groups. The biodegradation of SAA occurred through the breakdown of acetoacetyl groups, and the SAA separated into acetone, carbon dioxide, and starch. The degradation of starch subsequently took place. The initial biodegradation rate of SAA was low because of its hydrophobic nature, which was attributed to the slow hydrolysis of acetoacetyl groups. However, the BOD ratio of SAA in PLA/SAA was 6.9%, meaning that 3.3% of the PLA was biodegraded within 28 days. Thus, while SAA has a lower biodegradability rate than starch does, it can promote the marine biodegradability of PLA. PLA/SAA/End800 exhibited slightly lower biodegradability than did PLA/SAA. However, it exhibited biodegradation exceeding the BOD ratio of the SAA component within 28 days, as did the PLA/SAA. The results indicated that the cross-linked structures formed with enamines are also biodegradable. Enamine crosslinked structures have been reported to be hydrolytic and biodegradable [26, 47]. However, owing to the longer process required for enamine cross-linked SAA to be hydrolyzed to starch, the BOD of enamine cross-linked SAA was slightly lower than that of PLA/SAA [48, 49]. Although there is concern that the hydrophobic nature of amine-modified silicone interferes with the biodegradability of PLA/SAA, no significant effect was observed at the 3 phr addition level. In this blend, amine-modified silicone was not biodegradable, and a small amount of silicone is expected to remain in the ocean. Therefore, the environmental impact of this blend can be reduce further in the future by using biodegradable diamines as compatibilizers.

## Conclusions

SAA was synthesized as a reactive thermoplastic starch via transesterification. The synthesized SAA exhibited good thermoplasticity and was uniformly composited with PLA without a plasticizer. Amine-modified silicone was reacted with PLA and SAA to form a crosslinked structure during melt-kneading. The crosslinked structure inhibited PLA crystallization and significantly reduced the crystallinity of the blend. Although the amine-modified silicone was expected to bind to the PLA, it was excluded from the PLA lamellar crystals and did not affect the PLA crystal structure. The compatibility between PLA and SAA was significantly improved, and the toughness was enhanced with the addition of a small amount of amine-modified silicone (3 wt%). Furthermore, with respect to the morphology of the fracture surface, the interface between the SAA and PLA became indistinct, indicating that the dispersibility of the SAA in the PLA improved. Therefore, the amine-modified silicone functioned well as a compatibilizer for PLA and SAA and improved the mechanical properties of the blend. The performance of the compatibilizer was strongly dependent on the viscosity and amine equivalents of the amine-modified silicone. The PLA/SAA/amine-modified silicone blend showed marine biodegradability despite containing cross-linkers, which promoted the biodegradability of PLA. This approach can contribute to promoting the widespread use of biodegradable plastics as packaging materials and single-use plastics.

**Acknowledgements** This work was supported by Japan Science and Technology Agency Grants (JPMJPF2218), the Environment Research and Technology Development Fund JPMEERF21S11900 of the Environmental Restoration and Conservation Agency of Japan, and JSPS KAKENHI Grants (23H02024), JST PRESTO (JPMJPR23N4), and JST SPRING (JPMJSP2138).

**Author contributions** K.S.: Investigation, Writing - original draft, Writing - review & editing, Funding acquisition; Y.H. : Supervision, Writing -review & editing, Funding acquisition; H.U.: Supervision, Writing - review & editing, Funding acquisition.

**Funding** Open Access funding provided by Osaka University.

## Compliance with ethical standards

**Conflict of interest** The authors declare no competing interests.

**Publisher's note** Springer Nature remains neutral with regard to jurisdictional claims in published maps and institutional affiliations.

**Open Access** This article is licensed under a Creative Commons Attribution 4.0 International License, which permits use, sharing, adaptation, distribution and reproduction in any medium or format, as long as you give appropriate credit to the original author(s) and the source, provide a link to the Creative Commons licence, and indicate if changes were made. The images or other third party material in this article are included in the article's Creative Commons licence, unless indicated otherwise in a credit line to the material. If material is not included in the article's Creative Commons licence and your intended use is not permitted by statutory regulation or exceeds the permitted use, you will need to obtain permission directly from the copyright holder. To view a copy of this licence, visit http://creativecommons.org/licenses/by/4.0/.

## References

1. Carpenter EJ, Anderson SJ, Harvey GR, Miklas HP, Peck BB. Polystyrene Spherules in Coastal Waters. Science. 1972;178:749–50.
2. Ostle C, Thompson RC, Broughton D, Gregory L, Wootton M, Johns DG. The rise in ocean plastics evidenced from a 60-year time series. Nat Commun 2019;10:1622.
3. Borrelle SB, Ringma J, Law KL, Monnahan CC, Lebreton L, McGivern A, et al. Predicted growth in plastic waste exceeds efforts to mitigate plastic pollution. Science. 2020;369:1515–8.
4. Lambert S, Wagner M. Environmental performance of bio-based and biodegradable plastics: the road ahead. Chem Soc Rev 2017;46:6855–71.
5. Din MI, Ghaffar T, Najeeb J, Hussain Z, Khalid R, Zahid H. Potential perspectives of biodegradable plastics for food

packaging application-review of properties and recent developments. Food Addit Contam Part A 2020;37:665–80.
6. Singhvi MS, Zinjarde SS, Gokhale DV. Polylactic acid: synthesis and biomedical applications. J Appl Microbiol 2019;127:1612–26.
7. Madhavan Nampoothiri K, Nair NR, John RP. An overview of the recent developments in polylactide (PLA) research. Bioresour Technol 2010;101:8493–501.
8. Gorrasi G, Pantani R. Effect of PLA grades and morphologies on hydrolytic degradation at composting temperature: Assessment of structural modification and kinetic parameters. Polym Degrad Stab 2013;98:1006–14.
9. Iglesias-Montes ML, Soccio M, Luzi F, Puglia D, Gazzano M, Lotti N, et al. Evaluation of the factors affecting the disintegration under a composting process of poly(lactic acid)/Poly(3-hydroxybutyrate) (PLA/PHB) Blends. Polymers. 2021;13:3171.
10. Chotiprayon P, Chaisawad B, Yoksan R. Thermoplastic cassava starch/poly(lactic acid) blend reinforced with coir fibres. Int J Biol Macromol 2020;156:960–8.
11. Huang D, Hu Z-D, Liu T-Y, Lu B, Zhen Z-C, Wang G-X, et al. Seawater degradation of PLA accelerated by water-soluble PVA. E-Polym. 2020;20:759–72.
12. Diyana ZN, Jumaidin R, Selamat MZ, Ghazali I, Julmohammad N, Huda N, et al. Physical properties of thermoplastic starch derived from natural resources and its blends: a review. Polymers. 2021;13:1396.
13. Woźniak-Braszak A, Knitter M, Markiewicz E, Ingram WF, Spontak RJ. Effect of composition on the molecular dynamics of biodegradable isotactic polypropylene/thermoplastic starch blends. ACS Sustain Chem Eng 2019;7:16050–9.
14. Namphonsane A, Suwannachat P, Chia CH, Wongsagonsup R, Smith SM, Amornsakchai T. Toward a circular bioeconomy: exploring pineapple stem starch film as a plastic substitute in single use applications. Membranes. 2023;13:458.
15. Zhang H, Su Z, Wang X. Starch-based rehealable and degradable bioplastic enabled by dynamic imine chemistry. ACS Sustain Chem Eng 2022;10:8650–7.
16. Khatun A, Waters DLE, Liu L. A review of rice starch digestibility: effect of composition and heat-moisture processing. Starch - Stärke. 2019;71:1900090.
17. Averous L, Boquillon N. Biocomposites based on plasticized starch: thermal and mechanical behaviours. Carbohydr Polym 2004;56:111–22.
18. Fu J, Alee M, Yang M, Liu H, Li Y, Li Z, et al. Synergizing multiplasticizers for a starch-based edible film. Foods. 2022;11:3254.
19. Ali A, Xie F, Yu L, Liu H, Meng L, Khalid S, et al. Preparation and characterization of starch-based composite films reinfoced by polysaccharide-based crystals. Compos Part B Eng 2018;133:122–8.
20. Soni R, Asoh T-A, Hsu Y-I, Uyama H. Freshwater-durable and marine-degradable cellulose nanofiber reinforced starch film. Cellulose. 2022;29:1667–78.
21. Bai J, Pei H, Zhou X, Xie X. Reactive compatibilization and properties of low-cost and high-performance PBAT/thermoplastic starch blends. Eur Polym J 2021;143:110198.
22. Hu H, Xu A, Zhang D, Zhou W, Peng S, Zhao X. High-Toughness Poly(lactic Acid)/Starch Blends Prepared through Reactive Blending Plasticization and Compatibilization. Molecules. 2020;25:5951.
23. Noivoil N, Yoksan R. Compatibility improvement of poly(lactic acid)/thermoplastic starch blown films using acetylated starch. J Appl Polym Sci 2021;138:49675.
24. Gürler N, Paşa S, Hakkı Alma M, Temel H. The fabrication of bilayer polylactic acid films from cross-linked starch as eco-friendly biodegradable materials: Synthesis, characterization, mechanical and physical properties. Eur Polym J 2020;127:109588.
25. Denissen W, Rivero G, Nicolaÿ R, Leibler L, Winne JM, Du Prez FE. Vinylogous Urethane Vitrimers. Adv Funct Mater 2015;25:2451–7.
26. Sanchez-Sanchez A, Fulton DA, Pomposo JA. pH-responsive single-chain polymer nanoparticles utilising dynamic covalent enamine bonds. Chem Commun. 2014;50:1871–4.
27. Bhatia SK, Arthur SD. Poly(vinyl alcohol) acetoacetate-based tissue adhesives are non-cytotoxic and non-inflammatory. Biotechnol Lett 2008;30:1339–45.
28. Zare M, Ghomi ER, Venkatraman PD, Ramakrishna S. Silicone-based biomaterials for biomedical applications: Antimicrobial strategies and 3D printing technologies. J Appl Polym Sci 2021;138:50969.
29. Ma Z, Liu Z, Zou J, Mi H-Y, Liu Y, Jing X. Self-healable and Robust Silicone Elastomer for Ultrasensitive Flexible Sensors. ACS Sustain Chem Eng 2023;11:10496–508.
30. Liu H, Guo L, Tao S, Huang Z, Qi H. Freely Moldable Modified Starch as a Sustainable and Recyclable Plastic. Biomacromolecules. 2021;22:2676–83.
31. Weng T, He Z, Zhang Z, Chen Y, Zhou M, Wen B. A facile method of functional derivatization based on starch acetoacetate. Carbohydr Polym 2022;289:119468.
32. Hong L-F, Cheng L-H, Lee CY, Peh KK. Characterisation of physicochemical properties of propionylated corn starch and its application as stabiliser. Food Technol Biotechnol 2015;53:278–85.
33. Wang X, Huang L, Zhang C, Deng Y, Xie P, Liu L, et al. Research advances in chemical modifications of starch for hydrophobicity and its applications: A review. Carbohydr Polym 2020;240:116292.
34. El-Khodary E, Fukui Y, Yamamoto M, Yamane H. Effect of the melt-mixing condition on the physical property of poly(L -lactic acid)/poly(D-lactic acid) blends. J Appl Polym Sci 2017;134:45489.
35. Chen X, Zeng Z, Ju Y, Zhou M, Bai H, Fu Q. Design of biodegradable PLA/PBAT blends with balanced toughness and strength via interfacial compatibilization and dynamic vulcanization. Polymer. 2023;266:125620.
36. Fischer EW, Sterzel HJ, Wegner G. Investigation of the structure of solution grown crystals of lactide copolymers by means of chemical reactions. Colloid Polym. 1973;251:980–90.
37. Jariyasakoolroj P, Chirachanchai S. Silane modified starch for compatible reactive blend with poly(lactic acid). Carbohydr Polym 2014;106:255–63.
38. Ke T, Sun X. Melting behavior and crystallization kinetics of starch and poly(lactic acid) composites. J Appl Polym Sci 2003;89:1203–10.
39. Li H, Huneault MA. Comparison of sorbitol and glycerol as plasticizers for thermoplastic starch in TPS/PLA blends. J Appl Polym Sci 2011;119:2439–48.
40. Yang S, Wu Z-H, Yang W, Yang M-B. Thermal and mechanical properties of chemical crosslinked polylactide (PLA). Polym Test 2008;27:957–63.
41. Zhang J, Duan Y, Sato H, Tsuji H, Noda I, Yan S, et al. Crystal Modifications and Thermal Behavior of Poly(L -lactic acid) Revealed by Infrared Spectroscopy. Macromolecules. 2005;38:8012–21.
42. Hsieh Y-T, Nozaki S, Kido M, Kamitani K, Kojio K, Takahara A. Crystal polymorphism of polylactide and its composites by X-ray diffraction study. Polym J 2020;52:755–63.
43. Kawai T, Rahman N, Matsuba G, Nishida K, Kanaya T, Nakano M, et al. Crystallization and Melting Behavior of Poly (L -lactic Acid). Macromolecules. 2007;40:9463–9.
44. Marubayashi H, Asai S, Hikima T, Takata M, Iwata T. Biobased copolymers composed of L -lactic acid and side-chain-substituted lactic acids: synthesis, properties, and solid-state structure. Macromol Chem Phys 2013;214:2546–61.

45. Bagheri AR, Laforsch C, Greiner A, Agarwal S. Fate of so-called biodegradable polymers in seawater and freshwater. Glob Chall 2017;1:1700048.
46. Palai B, Mohanty S, Nayak SK. A comparison on biodegradation behaviour of polylactic acid (PLA) based blown films by incorporating thermoplasticized starch (TPS) and poly (Butylene Succinate-co-Adipate) (PBSA) biopolymer in soil. J Polym Environ 2021;29:2772–88.
47. Huang SJ, Ho L-H, Hong E, Kitchen O. Hydrophilic-hydrophobic biodegradable polymers: release characteristics of hydrogen-bonded, ring-containing polymer matrices. Biomaterials. 1994;15:1243–7.
48. Shibasaki K, Hsu Y, Uyama H. Facile Fabrication of Starch-Based UV Barrier Films with Remolding Ability and Reinforcement for Water Resistance. Macromol. Mater. Eng. 2024;309:2400137.
49. Li Q, Xiao X, Zhang X, Zhang W. Controlled synthesis of graft polymer through the coupling reaction between the appending β-Keto ester and the terminal amine. Polymer. 2013;54:3230–7.